Light Rotor: The 10-MW reference wind turbine

Bak, Christian; Bitsche, Robert; Yde, Anders; Kim, Taeseong; Hansen, Morten Hartvig; Zahle, Frederik; Gaunaa, Mac; Blasques, José Pedro Albergaria Amaral; Døssing, Mads; Wedel Heinen, Jens-Jakob

Total number of authors:
11

Published in:
Proceedings of EWEA 2012 - European Wind Energy Conference & Exhibition

Publication date:
2012

Document Version
Publisher's PDF, also known as Version of record

Light Rotor: The 10-MW reference wind turbine

*Christian Bak, Robert Bitsche, Anders Yde, Taeseong Kim, Morten H. Hansen, Frederik Zahle, Mac Gaunaa, José Blasques, Mads Døssing**

Jens-Jakob Wedel Heinen, Tim Behrens

DTU Wind Energy,
Risø Campus,
P.O.Box 49
4000 Roskilde, Denmark
chba@dtu.dk

Vestas Wind Systems A/S
Hedeager 44
8200 Aarhus N
Denmark
tibeh@vestas.com

Abstract

This paper describes the design of a rotor and a wind turbine for an artificial 10-MW wind turbine carried out in the Light Rotor project. The turbine called the *Light Rotor 10-MW Reference Wind Turbine (LR10-MW RWT)*, is designed with existing methods and techniques and serves as a reference to future advanced rotor designs in the project. The results shown in this paper are not for the final design, but for Iteration #2 in the design process. Several issues in the design process were highlighted.

Before carrying out the design many decisions have to be made and this paper elaborate on issues like the determination of the specific power and upscaling of the turbine.

The design of Iteration #2 of the *LR10-MW RWT* is carried out in a sequence between aerodynamic rotor design, structural design and aero-servo-elastic design. Each of these topics is described.

The results from the Iteration #2 design show a rather well performing wind turbine both in terms of power and loads, but in the further work towards the final design the challenges in the control needs to be solved and the balance between power performance and loads and between structural performance and mass will be investigated further resulting in changes in the present design.

Keywords: Wind turbine rotor, upscaling, airfoils, airfoil characteristics, structural design, aeroelastic design, aero-servo-elastic stability

1 Introduction

From the late 70'ies until now there has been a continuous upscaling of wind turbines. Further upscaling causes a challenge because the mass of the turbine increases with the cube of the rotor radius with linear upscaling. The largest wind turbines on the market or on the way to the market are in the order of 7 MW. However, increasing the size further will be even more challenging and for the rotor, new materials likely have to come into play if the existing layout will be used.

Therefore, the Light Rotor project has been initiated as a cooperation between DTU Wind Energy and Vestas, where the main objective is to change the design of the blades to increase the stiffness and overall performance of the rotor taking into account both aerodynamic, aero-servo-elastic and structural considerations. Thus, new airfoils and new aero-servo-elastic and structural methods are developed in the project. A very important activity in the project is to use a system approach in the overall design process, which includes further development of the existing tools within numerical optimization to establish an advanced design complex.

An upscaling to obtain a light weight rotor is managed by increasing the thickness to chord ratio of airfoils along the blade span and adjusting the thickness of load carrying structural elements in the blade, rather than just keeping relative thicknesses and adjusting the thickness of load carrying elements. The impact of increasing the thickness ratio along the blade is that the weight and edgewise loads scale better with the flapwise loads while considering the negative impact from higher thickness ratio on power and thrust.

As part of the Light Rotor project a 10-MW reference rotor is designed, so that future designs in the project can be compared to this rotor, also called the *Light Rotor 10-MW Reference Blade (LR10-MW blade)*.

**Mads Døssing made a significant contribution to the aerodynamic rotor design, but is not part of DTU Wind Energy anymore*

Even though the focus in the project is the rotor design, the existence of the entire wind turbine is needed to understand the rotor performance in its interaction with the entire system including the structural dynamics of the blades, the tower and the drivetrain. The 10-MW wind turbine used to reveal the performance of the blade, the *Light Rotor 10-MW Reference Wind Turbine (LR10-MW-RWT)*, is inspired by the artificial 5-MW reference wind turbine [1], but the rotor is designed from scratch. Even though new methods are developed in the Light Rotor project the methods used for designing the 10-MW reference blades are the existing ones to also reveal the effect of using updated methods in the rotor design process later in the project. Thus, the blade weight will be minimized using existing methods, but no new concepts or materials will be used. Therefore, a significant reduction in mass is not expected compared to existing upscaled blades.

The design of the *LR10-MW-RWT* needs several iterations from airfoil choices to aeroelasitc design. The design presented in this paper is not the final one, but Iteration #2.

2 Methods

The design method is based on an iterative trial-and-error method, where one design is developed in the way as sketched in Figure 1. Thus, the design is analyzed either aerodynamically, structurally or aeroelastically and if the design is not fulfilling the requirements it is brought at least one step back in the process.

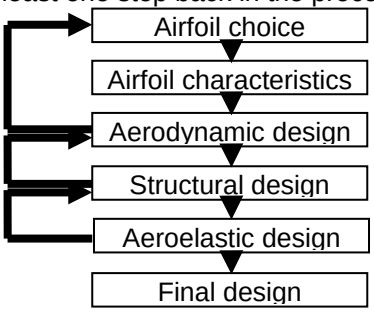

Figure 1: Sketch of design procedure

This design process is in contrast to the method that is going to be developed in the Light Rotor project, where a system approach will be developed and used, but for the design of the reference rotor only the existing methods are used as shown, to reflect the capability of the state-of-the-art methods and tools at the project start.

2.1 Basic considerations

As is the trend in the design for many new large wind turbines and in line with the strategy in EU the wind turbine is designed for offshore operation. This is the reason for basing the design on class IA according to IEC-61400-1 standard.

Determining the rotor diameter is of primary importance when designing a new wind turbine. The rotor size has a significant impact on power and loads and therefore also on the cost. Analyzing Vestas IEC class I designs for offshore applications and the artificial 5-MW reference turbine [1] show the specific power, which are normalized entities reflecting the sizing of the generator and the rotor in combination, Table 1. It is seen that the specific power is varying for the selected designs between 305W/m^2 and 472W/m^2. Whether the specific power should be small or big depends on the specific cost function for the turbine/manufacturer.

Table 1: Specific power for different IEC class I designs for high wind

Turbine	V90-3.0MW	V112-3.0MW	V164-7.0MW	Artificial 5MW reference
Specific power [W/m^2]	472	305	331	407

To be able to compare in terms of upscaling issues, the size of the 10-MW rotor was based on the artificial 5-MW rotor [1] and therefore had identical specific power. Thus, it was upscaled to a radius of 89.17m with a blade length of 86.37m assuming that the hub radius is 2.8m.

Furthermore, it is important to estimate an order of magnitude for the expected mass of the blade. Data for a few blades are shown in Table 2 to reveal the mass in case of direct upscaling, where the blades are designed with varying combinations of glass, carbon fibers and/or balsa.

Furthermore, the rest of the turbine was upscaled from the artificial 5MW reference turbine [1] applying the classical similarity rules [2]. This is based on assumptions of geometrical similarities. It means that in order to achieve twice as much power output the rotor area has to be doubled.

Table 2: The mass of selected blades and the mass in case of direct upscaling

Blade	V112-3.0MW	V164-7.0 MW	LM73.5P-6MW	Artificial 5MW reference
Mass of blade [tons]	11.9	35	26	17.6
Mass of blade directly upscaled to radius 89.17m [tons]	48	45	43	50

The weight and the power is scaled by $m \cdot f_s^3$ and $P \cdot f_s^2$, respectively, where f_s is the geometric scaling factor obtained by $f_s = \sqrt{(10/5)}$. All geometric properties are scaled linearly by $L \cdot f_s^1$ and the 1st Mass Moment of Inertia is scaled by $I \cdot f_s^4$ and the 2nd Mass Moment of Inertia is scaled by $I \cdot f_s^5$. The method neglects second-order aerodynamic effects and assumes linear structural behavior, and is based on the idea that the stresses due to aerodynamic loading is invariant during upscaling, whereas loading due to weight is linearly increasing with the scaling factor.

One of the weaknesses by this method is that it may lead to a higher RNA (Rotor Nacelle Assembly) mass than expected in very large wind turbine designs depending on the scaled turbine. According to the scaling theory the RNA mass of the 5MW reference wind turbine scaled to the same rotor size as the Vestas V164-7.0 MW turbine will have an increase of approximate 55% in weight compared to the specifications. The over estimation is primarily due to a very high nacelle and hub mass as the blade weight is only overestimated by 11%. Therefore, the nacelle and hub masses and inertias have been reduced in the design of the upscaled *LR10-MW-RWT* wind turbine. This is done by scaling the nacelle and hub mass of the Vestas V164-7.0 MW and scaling inertias to the same levels as an equal weighing component of the scaled 5MW reference turbine.

2.2 Airfoil choice

Many different airfoils exist and can potentially be selected for the blade design. However, on the blade for the 10-MW turbine special consideration should be put on decreasing the weight and one important way is to increase the relative thickness of the airfoils to stiffen the blade. Thus, the airfoils used in the design need to be medium thick to thick. However, only rather few airfoils series exist with the weight on high relative thickness. Thus, the FFA airfoils [3], the DU airfoils [4] and the Risø airfoils [5,6] can be used. It is chosen that the blade is designed using the FFA-W3-xxx series since these airfoils are publically available, are fairly aerodynamically efficient and have specific focus on high relative thickness. However, thicker airfoils are in general less aerodynamic efficient, which result in a reduction in power. Thus, caution should be taken when using thicker airfoils.

2.3 Airfoil characteristics

The airfoil characteristics for the FFA-W3 series should preferably be based on wind tunnel tests. However, the existing wind tunnel measurements from 1998 are carried out at a Reynolds number of $Re = 1.6 \times 10^6$ [7] and at a relatively high turbulence intensity. Because the influence on the aerodynamics from the Reynolds number is significant, XFOIL computations [8] have been carried out at Reynolds numbers between 9×10^6 and 13×10^6 to establish a set of airfoil characteristics, which are as well corrected for 3D effects [9]. These airfoil characteristics take into account the effect of surfaces that are both clean and contaminated by weighting the two different performances.

2.4 Aerodynamic design

The aerodynamic rotor design is based on the numerical optimization tool HAWTOPT [10]. With this tool a rotor was aerodynamically optimized with many design variables along the blade span in terms of chord length, relative thickness and twist. Furthermore, constraints were set on the absolute thickness. With the rotor of the 5MW reference turbine as the starting point it was decided to increase the absolute thickness slightly to stiffen the rotor. Also, it was decided not to increase the relative thickness to more than 24.1% on the outer part of the blade, because experience has shown that the roughness sensitivity increase and the aerodynamic airfoil performance decrease significantly with increasing relative airfoil thickness above 24-27%. It was chosen that the maximum tip speed should be 80m/s and

the design tip-speed ratio should be 8.06. With this as a design basis the blade was designed with the FFA-W3-241 airfoil from appr. 2/3 radius to the tip, and with thicknesses increasing from appr. 2/3 radius towards the root. In the design, loads from high wind speeds were taken into account by constraining the loads at stand-still, which e.g led to a rather slender blade. Furthermore, the maximum chord length was set to 6.0m. The thrust in normal operation was considered by investigating the relation between power, thrust and blade root flap moments. Thus, the power coefficient could be slightly higher for this blade if higher thrust and blade root moments were allowed.

2.5 Structural design

A complete description of the blade's external and internal geometry and composite layup was generated in the form of a finite element shell model (~600000 degrees of freedom), Abaqus 6.11 [11]. Figure 2 shows two views of the blade. For the purpose of composite layup definition the blade was partitioned into 52 regions radially (see Figure 2) and 10 regions circumferentially (see Figure 4). Three types of glass fiber/epoxy laminates were used (uniaxial, biaxial and triaxial laminates) together with PVC foam as sandwich core material. The structural design is based on a classical approach using a load carrying box girder with two shear webs and sandwiches for the leading and trailing edge panels. The caps were approximately placed at the maximum thickness of the airfoil in order to obtain maximum flapwise bending stiffness. While the cap width (which is also the distance between the shear webs) varies along the length of the blade, the axis of the box girder is a straight line, as shown in Figure 3. Trailing and leading edge reinforcements were used in order to increase edgewise bending stiffness and prevent buckling of the trailing edge, see Figure 4. The finite element shell model of the blade was used to compute local stresses and strains, natural frequencies, and to perform buckling analysis. The mass of one blade is 47900 kg, which is the mass of the composite laminates and core materials, not including the mass of any metallic structures or adhesives. In the design process one focus is to reduce this mass, but it seems that the mass is somewhat high compared to a direct upscaling of the V164-7.0MW and the LM73.5P blade. However, it should be noticed that the *LR10-MW blade* is made only of glass fiber and not carbon fiber and/or balsa in contrast to many new blades.

2.6 Aeroelastic design

Based on the aerodynamic and structural design, 2D cross-sectional data from the 3D blade design is extracted using the recently developed cross-section analysis software BECAS [12]. The input for BECAS is generated based on the information contained in the finite element shell model using an automatic process. This guarantees consistency between the different models. The cross sectional data is used for 1D beam analysis for HAWCStab2 [13], the aero-servo-elastic stability tool, and HAWC2 [14], the aeroelastic tool. The other structural properties for foundation, tower, drivetrain, and hub are obtained by the upscaling manner described in section 2.1. The load predictions of the designed turbine are very important because the designed blade and turbine have to be able to withstand all loadings experienced during its life time. The considered load cases (Table 3) are selected based on the IEC 61400-1 standard [15]. In Table 3 DLC 1.1 and DLC 1.3 are normal power production cases with normal turbulence model and extreme turbulence model, respectively.

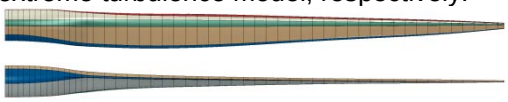

Figure 2: Blade seen from suction side (top) and trailing edge (bottom).

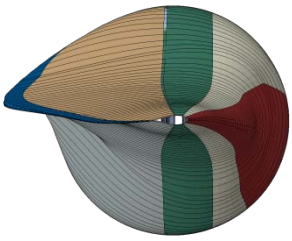

Figure 3: Blade seen from the tip.

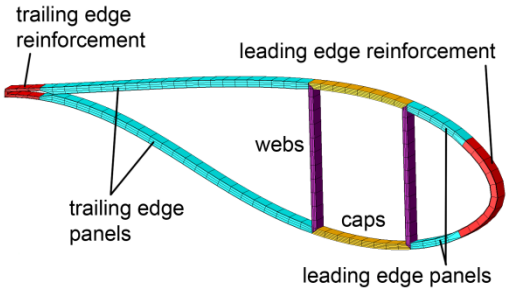

Figure 4: Blade cross-section.

Table 3: Design load cases according to IEC standard [15]

#	Load case	DLC#
1	Power production	1.1, 1.3
2	Power production with occurrence of fault	2.1, 2.3
3	Start up	3.2
4	Normal shut down	4.1, 4.2
5	Emergency shut down	5.1
6	Stand-still	6.1 – 6.3

DLC 2.1 and DLC 2.3 are normal power production cases including system faults (control system, grid system, protection system etc.) with normal turbulence model and extreme operating gust, respectively. DLC 3.2 is a turbine start up condition with extreme operating gust. DLC 4.1 and DLC 4.2 are a turbine normal shut down condition with normal wind profile model and extreme operating gust. DLC 5.1 is a turbine emergency shut-down condition with normal turbulence model. Finally, DLC 6.1, DLC 6.2, and DLC 6.3 are stand-still condition with extreme wind speed model for which 50-year recurrence period wind speed model without (DLC 6.1) and with (DLC 6.2) grid fault condition and 1-year recurrence period wind speed model with extreme yaw misalignment (DLC 6.3).

The loads during the turbine life time are investigated and the maximum loads along the blade span as well as the maximum blade tip deflection are given as input to the structural design step. This process is continued while both structural design and aeroelastic design are satisfied.

3 Results

The design of the *LR10-MW blade* requires several iterations between aerodynamic design, structural design and aero-servo-elastic design as sketched in Figure 1. It is not known from the start of the design process how many iterations will be needed. In this section the results from Iteration #2 in the design process are presented. Thus, the aerodynamic, structural and aero-servo-elastic design is not entirely finalized because it was assessed that it can be optimized further, especially in the interaction with the rest of the wind turbine and the control.

3.1 Aerodynamic design and performance

The aerodynamic rotor design is the starting point in the blade design. Even though the blade seems to be rather aerodynamically efficient it is likely that some changes are needed before the final design. The Iteration #2 design is compared to the blade of the 5MW reference wind turbine in Figure 5. It is seen that compared to the 5-MW RWT the blade is somewhat more slender and the absolute thickness is slightly higher. In Figure 6 and Figure 7 a few parameters reflecting the aerodynamic performance are shown. Compared to the 5-MW reference rotor it is slightly less efficient, which probably is due to the thicker airfoils. This will be investigated further in the next design iterations.

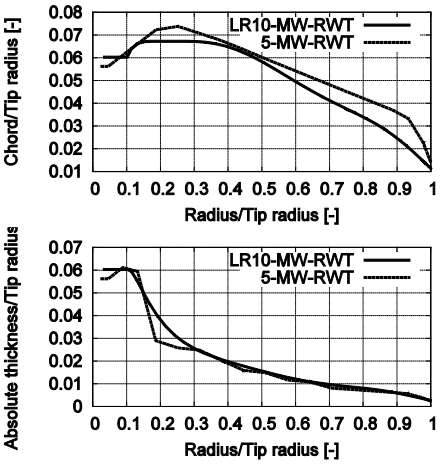

Figure 5: Normalized chord and thickness for the LR10-MW blade compared to the artificial 5-MW blade

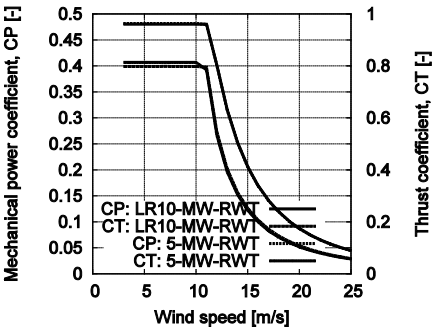

Figure 6: Power and thrust coefficient vs. wind speed for the LR10-MW rotor and the 5-MW rotor.

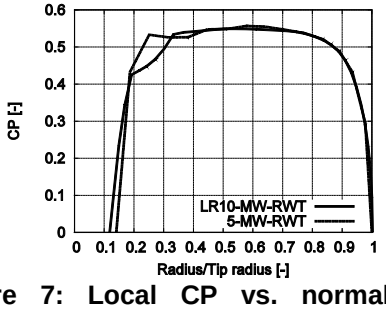

Figure 7: Local CP vs. normalized radius for the LR10-MW rotor and the 5-MW rotor.

3.2 Structural performance

As an example for the cross section stiffness properties computed by BECAS the bending stiffness and the torsional stiffness are shown in Figure 8 and Figure 9, respectively. The natural frequencies and corresponding mode shapes of the blade were computed using the finite element shell model. The first 6 are listed in Table 4. The first torsional mode is found as mode number 6. Ultimate bending moment curves were derived by determining the highest (flapwise or edgewise) bending moment that occurred at any point in time (in any load case) at a number of radial positions. These "virtual" load cases were used as a basis for strength and buckling analysis using the finite element shell model. As an example Figure 10 shows the longitudinal strain in the pressure side and suction side cap under ultimate flapwise bending moments. The strains are below allowable limits considering typical ultimate compressive and tensile strains and typical partial safety factors for loads and materials.

Buckling calculations were performed using eigenvalue buckling analysis. Throughout the design process local buckling phenomena were mainly an issue for the caps close to the tip (where the thickness of the caps is less dictated by bending stiffness considerations), and at the trailing edge. At the trailing edge the buckling problem was solved by additional reinforcement layers and sandwich principles.

3.3 Aeroelastic performance

As a first step in the evaluation of the aero-servo-elastic performance of the *LR10-MW-RWT*, an aeroelastic stability analysis was performed with HAWCStab2. To validate the structural blade model in HAWC2 and HAWCStab2 based on prismatic Timoshenko beam elements and from BECAS, Table 5 lists the natural frequencies of the structural blade modes up to first torsion, which is mode number 7 in the beam model. It seems that the edgewise bending modes have somewhat higher frequencies than in the shell model when comparing to Table 4. For the aeroelastic stability analysis, the mean operational pitch angles are computed with HAWCStab2 for each wind speed in the range from 3 m/s to 25 m/s.

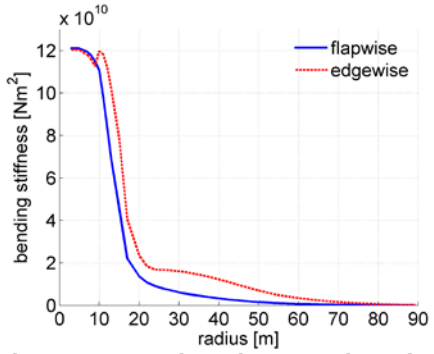

Figure 8: Flapwise and edgewise bending stiffness distribution.

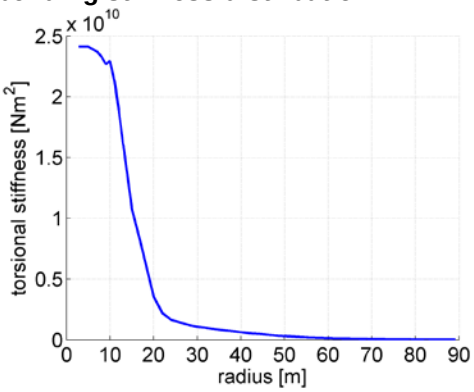

Figure 9: Torsional stiffness distribution.

Table 4. Natural frequencies and mode shapes.

Mode Number	*Frequency [Hz]*	*Remark*
1	0.5210	First flapwise
2	0.8820	First edgewise
3	1.6142	Second flapw.
4	2.8173	Second edgew.
5	3.4027	Third flapwise
6	5.0342	First torsional

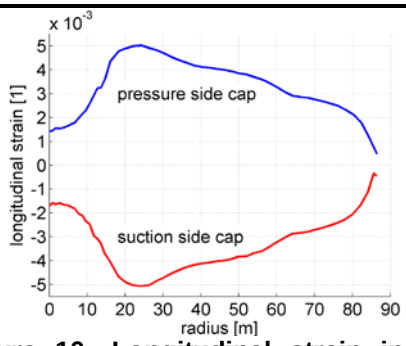

Figure 10: Longitudinal strain in the pressure side and suction side cap under ultimate flapwise bending moments.

The mean rotor speed is simply obtained from a prescribed tip speed ratio of 9, which is slightly higher than the design value to avoid stall of the blades in high turbulence and other complex inflow

conditions. The generator speed is limited between 589.54 rpm and 1173.7 rpm, and the gear ratio is 137.2, yielding a maximum rotor speed of 8.56 rpm. For each set of wind speeds and rotor speeds, the optimal collective pitch angle is computed with HAWCStab2 including elastic deflections of the blades, whereby the mean chord twist changes.

Table 5. Natural frequencies of blade modes computed with HAWCStab2.

Mode Number	*Frequency [Hz]*	*Remark*
1	0.57	First flap
2	0.95	First edge
3	1.63	Second flap
4	3.06	Second edge
5	3.34	Third flap
6	5.46	Fourth flap
7	5.77	First torsion

Figure 11 shows the pitch angles and rotor speeds used in the following stability analysis. These mean pitch angles are deduced from the optimal pitch angles computed with HAWCStab2 by setting a minimum pitch angle of 0 deg. To show the effect of the blade deformation the optimal pitch obtained for rigid and flexible blades are shown. Figure 12 shows the mean aerodynamic power computed with HAWCStab2 for the used and the optimal pitch angles, showing slightly lower power around the rated wind speed.

Figure 13 shows the local blade torsion at five different wind speeds (top plot) and blade tip deflections (bottom plot) computed with HAWCStab2. Torsion is defined positive towards stall. Compared to other large blades, the reference blade seems to be quite stiff in torsion. The maximum flapwise tip deflections were also quite low, below the typical 10% of the blade length.

Figure 14 and Figure 15 show the aero-elastic modal frequencies and damping ratios of the first eight turbine modes for a stationary mean operation at the wind speeds, rotor speeds and pitch angles shown in Figure 11. The frequencies of modes that involve significant motion of the blades depend on the operational wind speed due to the variation of rotor speed and collective pitch angle, whereas the tower and drivetrain (DT) modal frequencies are almost unaffected by the change of operational conditions. The aeroelastic damping ratios in Figure 15 show the high damping of flapwise modes due to their direct coupling of changes in angle of attack. The reduced flapwise damping around rated wind speeds are caused by operations closest to the critical angle of attack. The first longitudinal tower bending mode is also highly damped, whereas modes that involve mainly inplane blade motions are low damped by the aero-dynamic forces. The lowest damped mode in open-loop is the lateral tower mode.

The next step in the evaluation of the aero-servo-elastic performance of the *LR10-MW-RWT* is the tuning of the Risø controller [16,17]. This controller is based on two PID regulators; one that regulates generator speed below rated using generator torque to follow a desired speed profile for each wind speed based on a first order filtered nacelle wind speed signal with sufficiently long time lag to avoid fluctuations from the disturbed flow. The generator speed profile is given by its max/min values and a tip speed ratio of 9 which is higher than its optimal value to avoid blade stall in sheared and turbulent inflow. Above rated wind speed, the other PID regulator keeps the rotor speed at its rated value using collective pitch. The gains of this regulator are gain scheduled to handle variations of the aerodynamic gain of the rotor torque as the wind speed increased. The gain tuning of both regulators are done automatically using HAWCStab2. The switching between the two regulators in this Risø controller is based on the measured electrical power and collective pitch angle in combination with appropriate filters. The measured generator speed used in both speed regulators is second order low-pass filtered to avoid excitation of the free-free drivetrain mode at 0.58 Hz. To check the controller performance, Figure 16 shows selected results of a HAWC2 simulation of a full range wind step case from 5 m/s to 25 m/s without turbulence and wind shear. Note the similarity with the steady state values from HAWCStab2 (cf. Figure 11, Figure 12, and Figure 13). Note also that there are some large variations of the signals after 350 s at 11 m/s just below the rated wind speed. These variations are caused by the switching between the two regulators. Current work will remove these variations in final descriptions of the *LR10-MW-RWT*.

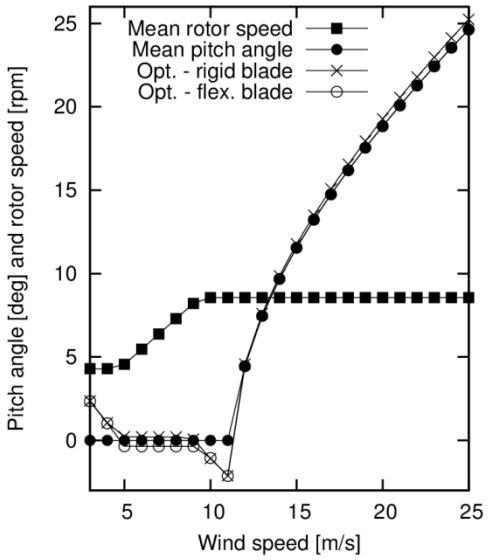

Figure 11: Mean pitch angles and rotor speeds used in the aeroelastic stability analysis (solid points). Optimal pitch angles shown for rigid (×) and flexible (o) blades.

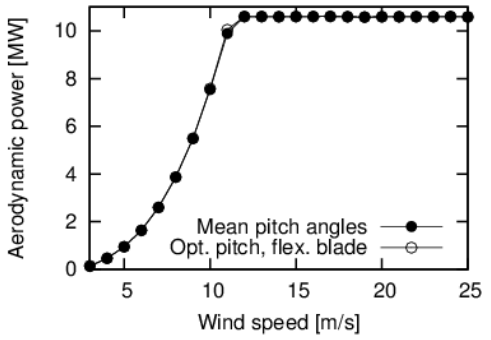

Figure 12: Aerodynamic power obtained from HAWCStab2 for used and optimal pitch angles including blade deflections.

Based on the tuned controller selected load cases are performed with HAWC2. Figure 17 shows the maximum blade flapwise and edgewise loads according to each load case. It is observed that the power production with extreme turbulence model (DLC1.3) produces the biggest loads on the blade for both flapwise and edgewise loading. Therefore this design load case should be considered as a design load case. All obtained loads are going to be transferred to the structural analysis step in order to investigate if the designed structural configuration is able to withstand the maximum loads obtained.

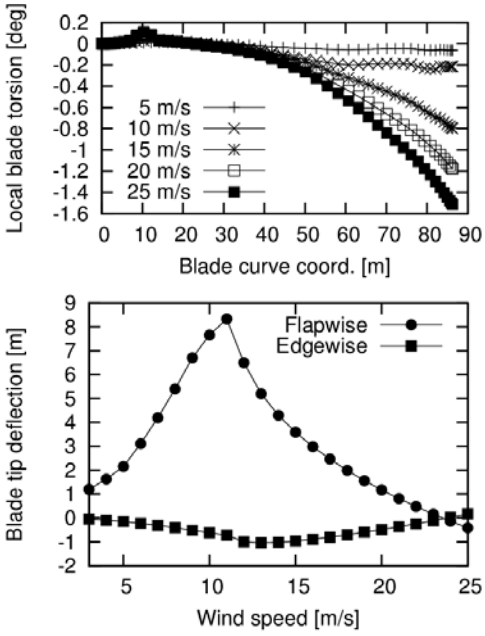

Figure 13: Mean local blade torsion at five different wind speeds (top) and blade tip deflections (bottom) from HAWCStab2.

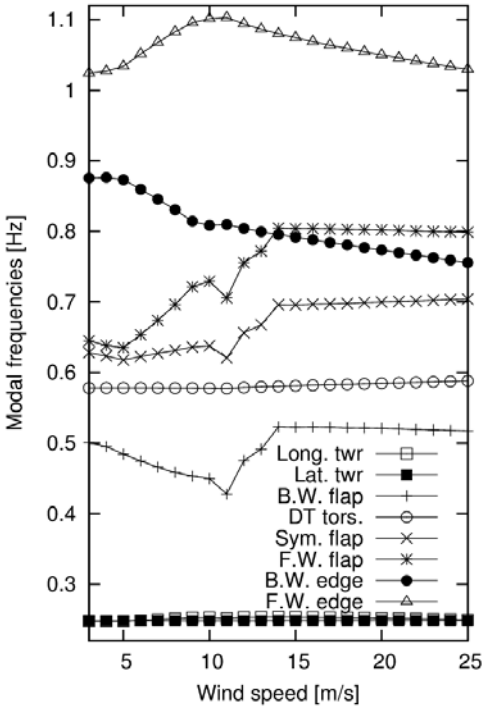

Figure 14: Open-loop modal frequencies of the first eight aeroelastic modes of the 10MW reference turbine. BW and FW denote backward and forward whirling.

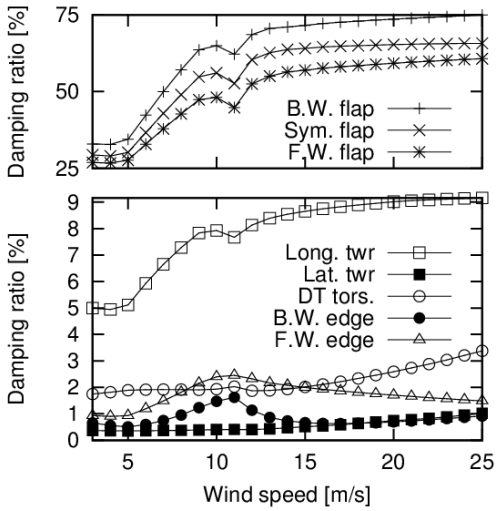

Figure 15: Open-loop damping ratios of the first eight aeroelastic modes of the 10MW reference turbine.

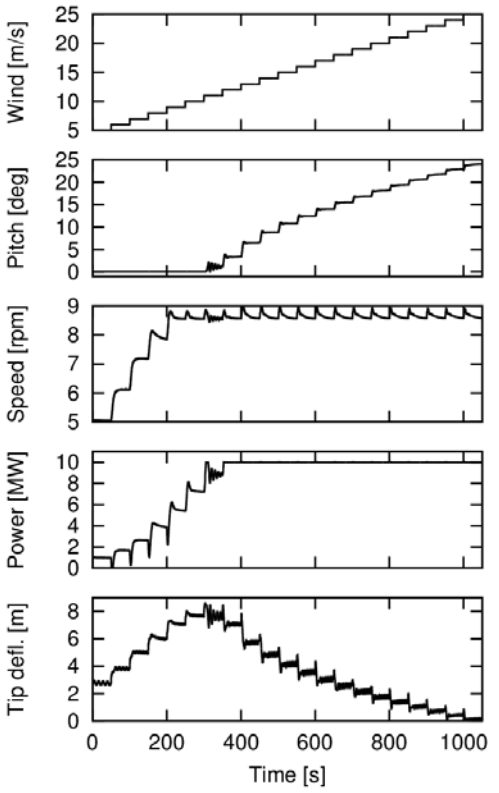

Figure 16: Simulation with HAWC2 of a wind step case to check controller performance. Gravity is included but turbulence and wind shear are neglected.

Figure 18 shows the blade maximum tip deflections for all load cases considered.

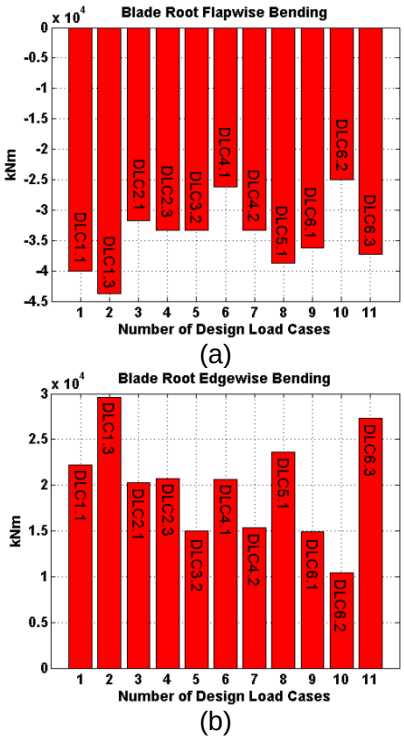

Figure 17: Maximum blade root bending moments; (a) flapwise bending moment (b) edgewise bending moment.

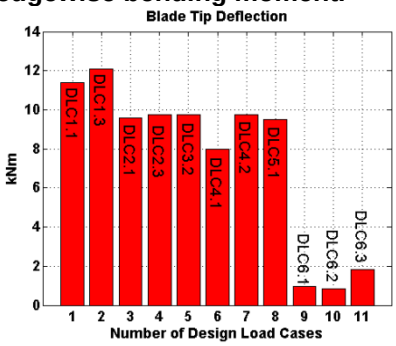

Figure 18: Max. blade tip deflections.

The tip clearance of the *LR10-MW-RWT* is approximately 14.9m (where 5deg tilt angle and 2.5deg coning angle of the rotor are taken into account). The maximum blade tip deflection obtained is approximately 12.4m from DLC 1.3 case. Therefore it may conclude that the current blade design is acceptable in terms of the blade clearance.

4 Conclusions

This paper showed the design of a rotor and a wind turbine for a 10-MW wind turbine carried out in the Light Rotor project. Even though the project focuses on rotor design, it is of primary importance to design the rotor together with the entire system: Foundation, tower, drivetrain and rotor. The results shown in the paper are not for the final design, but for Iteration #2

in the design process. Thus, the design process will need more iterations between aerodynamic, structural and aeroelastic design. However, even for this Iteration #2 design several issues were highlighted. Selecting the specific power is not trivial and depends on the cost function for the manufacturer. For this rotor it was chosen to maintain the specific power of the artificial 5-MW wind turbine. Furthermore, the upscaling laws tend to overestimate the mass of the nacelle and drivetrain. Thus, the mass of the nacelle and drivetrain was reduced relative to the artificial 5-MW wind turbine. Also, it seems that the mass of the *LR10-MW blade* is somewhat too high compared to blades directly upscaled from V164-7.0MW and LM73.5P. However, this is likely because no carbon fiber or balsa and only glass fiber is used for the *LR10-MW blade*. In the further work towards a final design, the challenges in the control needs to be solved and the balance between power performance, loads and structural layout will be investigated further resulting in changes in the present design. Finally, this work has learned that expert knowledge is vital for solving specific challenges in the design, but that general knowledge in the blade design process is equally important to take optimum decisions.

5 Availability of the design

The described wind turbine is Iteration #2 in the design of the 10 MW reference wind turbine. The final wind turbine design with all details in the design will be available at www.vindenergi.dtu.dk under the menu *Research* from July 1, 2012.

6 Acknowledgements

This project was funded partly by the Danish Energy Agency by the project EUDP2010-I Light Rotor, and partly by eigenfunding from the project partners.

References

[1] Jonkman J, Butterfield S, Musial W, Scott G. “Definition of a 5-MW Reference Wind Turbine for Offshore System Development”. Technical Report NREL/TP-500-38060, NREL National Renewable Energy Laboratory 2009.

[2] P.K.Chaviaropoulos, Similarity Rules for W/T Up-Scaling, UpWind report, CRES, April 2006

[3] Björk A. Coordinates and calculations for the FFA-w1-xxx, FFA-w2-xxx and FFA-w3-xxx series of airfoils for horizontal axis wind turbines. Ffa tn 1990-15, FFA, Stockholm, Sweden, 1990

[4] Timmer W.A. and van Rooij R.P.J.O.M. Summary of the delft university wind turbine dedicated airfoils. Proc. AIAA-2003-0352, 2003

[5] Fuglsang P. and Bak C. Development of the Risø wind turbine airfoils. Wind Energy, 7:145-162, 2004.

[6] Bak*, C.;* Andersen*, P.B.;* Madsen*, H.A.*, Gaunaa*, M.; ”*Design and Verification of Airfoils Resistant to Surface Contamination and Turbulence Intensity”, AIAA 2008-7050, 26th AIAA Applied Aerodynamics Conference, 18 - 21 August 2008, Honolulu, Hawaii

[7] Fuglsang, P.; Antoniou, I.; Dahl, K.S.; Madsen, H.A.; ”Wind tunnel tests of the FFA-W3-241, FFA-W3-301 and NACA 63-430 airfoils”, Risø-R-1041(EN), Risø National Laboratory, Roskilde, Denmark, December 1998

[8] Drela M. XFOIL, An Analysis and Design system for Low Reynolds Number Airfoils. Low Reynolds Number Aerodynamics, volume 54. In Springer- Verlag Lec. Notes in Eng., 1989.

[9] Bak, C.; Johansen, J.; Andersen, P.B.; “Three-Dimensional Corrections of Airfoil Characteristics Based on Pressure Distributions”, Presented at the European Wind Energy Conference & Exhibition (EWEC), 27. Feb. – 2. Mar. 2006, Athens, Greece

[10] Fuglsang, P.; Thomsen, K., Site-specific design optimization of 1.5-2.0 MW wind turbines. J. Solar Energy Eng. (2001) **123** , 296-303

[11] Abaqus Analysis User's Manual, Abaqus 6.11 Online Documentation, Dassault Systèmes, 2011

[12] Blasques J.P. “User’s Manual for BECAS - A cross section analysis tool for anisotropic and inhomogeneous beam sections of arbitrary geometry”, Technical Report Risø-R 1785, Risø 2011.

[13] Hansen, M. H., “Aeroelastic properties of backward swept blades”, In the Proceedings of 49th AIAA Aerospace Sciences Meeting Including The New Horizons Forum and Aerospace Exposition, Orlando, 4-7 January, 2011

[14] T. J. Larsen, H. Aa. Madsen, A. M. Hansen, and K. Thomsen. Investigations of stability effects of an offshore wind turbine using the new aeroelastic code HAWC2. Proceedings of the conference ”Copenhagen Offshore Wind 2005”, 2005.

[15] International Standard, IEC 61-400-1, 3rd edition. Wind turbines – Part 1: design requirements.

[16] T. J. Larsen and T. D. Hanson, “A method to avoid negative damped low frequent tower vibrations for a floating, pitch controlled wind turbine”, The Science of Making Torque from Wind, Journal of Physics: Conference Series 75, IOP Publishing, 2007.

[17] T. J. Larsen, H. Aa. Madsen, G. Larsen, K. S. Hansen, ”Validation of the Dynamic Wake Meander Model for Loads and Power Production in the Egmond aan Zee Wind Farm”, (Submitted), 2012.